
From Priors to Perception: Grounding Video-LLMs in Physical Reality

Zicheng Zhao

Shanghai Jiao Tong University
zzcsjtu7@sjtu.edu.cn

Chaofan Gan

Shanghai Jiao Tong University
ganchaofan@sjtu.edu.cn

Shijie Li

Shanghai Jiao Tong University
shijieli@sjtu.edu.cn

Weiyao Lin

Shanghai Jiao Tong University
wylin@sjtu.edu.cn

Abstract

While Video Large Language Models (Video-LLMs) excel in general understanding, they exhibit systematic deficits in fine-grained physical reasoning. Existing interventions not only suffer from limited generalization but fundamentally conflate generative artifacts with genuine physical fallacies. Furthermore, we find that models fail systematically not only in *anti-physics* anomalies but also in *counter-intuitive* scenarios where visual facts contradict statistical expectations. Accordingly, we propose the Unified Attribution Theory: this dual failure stems not from perception deficiency, but from Semantic Prior Dominance—the reasoning mechanism is deeply hijacked by internal narrative scripts. To address this, we construct the Programmatic Adversarial Curriculum (PACC), the first high-fidelity adversarial video dataset synthesized based on physical laws, thoroughly decoupling visual artifacts from logical errors. Concurrently, we design the Visual-Anchored Reasoning Chain (VARC) to force models to explicitly ground their judgments in low-level visual facts prior to logical adjudication. Experiments demonstrate that without invasive architectural modifications, standard LoRA fine-tuning with the PACC curriculum effectively neutralizes prior interference in state-of-the-art (SOTA) models, yielding a substantial leap in physical reasoning capabilities.

Code: <https://github.com/LiamZhao326/From-Priors-to-Perception>.

1 Introduction

Although Video Large Language Models (Video-LLMs) excel in general video understanding [21, 23], they exhibit severe deficits in fine-grained physical reasoning [24, 20]. Existing SOTA models fail to identify obvious physical violations (e.g., object levitation and rigid-body penetration) [1, 24], exposing a fundamental weakness: models merely overfit visual-textual correlations rather than reasoning from underlying physics [20]. As AI advances toward World Models [4] and Embodied AI [48], such cognitive deficits threaten reliable scene simulation and real-world interaction by trapping models in superficial 2D fitting. Breaking this physical reasoning bottleneck is an imperative step toward genuine real-world understanding.

To investigate the root cause of these failures, we expose the model’s systematic fallacies through a “ball-and-domino” interaction scenario (Fig. 1a). In an *anti-physics* setting where dominoes fall without contact from the ball, the model fabricates invisible forces, driven by the logical prior that “the world must conform to common sense” to forcefully rationalize the fallacy. Furthermore, we find this mechanism also causes failures in physically plausible yet *counter-intuitive* real-world scenarios:

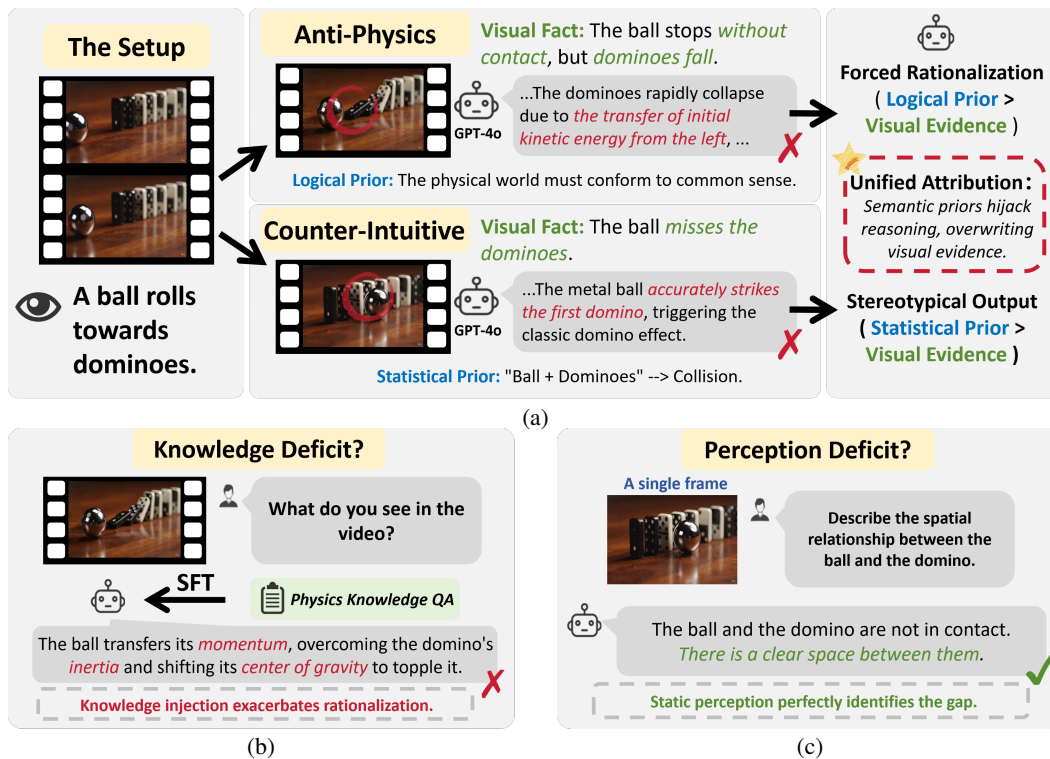


Figure 1: **Illustration of Semantic Prior Dominance.** (a) SOTA models (e.g., GPT-4o [26]) exhibit dual failures: logical priors drive forced rationalizations in *anti-physics* scenarios, while statistical priors trigger stereotypical outputs in *counter-intuitive* cases. Pilot studies (VideoLLaMA3 [43]) rule out knowledge or perception deficits: (b) injecting physical knowledge exacerbates erroneous rationalizations; (c) single-frame tests confirm intact spatial perception. Thus, semantic priors hijack reasoning, overriding objective visual evidence.

when the ball misses the dominoes, the model ignores the objective gap and succumbs to the statistical prior of a “ball-domino collision,” resulting in a *what-it-expects-is-what-it-sees* stereotypical output. Pilot studies rule out the model’s knowledge or perception deficits: injecting physical knowledge exacerbates the anti-physics misjudgment (Fig. 1b), whereas a single-frame test proves the model precisely identifies the visual gap, confirming intact low-level perception (Fig. 1c).

Accordingly, we propose the **Unified Attribution Theory**: the aforementioned dual failures are essentially different manifestations of **Semantic Prior Dominance**. Although the vision encoder remains robust, the reasoning mechanism is deeply hijacked by internal narrative scripts. Unlike recent works that merely observe narrative-level hallucinations (e.g., NOAH [17]), we expose a deeper vulnerability: prior dominance directly paralyzes the model’s capacity to ground low-level physical facts, forcing it to overwrite objective visual evidence with subjective expectations.

While existing works try to alleviate physical reasoning deficits through interventions like inference-time decoding and reinforcement learning [39, 20], or invasive architectural modifications with heavy computational overhead and extremely poor generalization [24, 42], they fail to resolve the root cause of semantic prior hijacking. Critically, data paradigms relying on passive anomaly capture from generative models conflate low-level visual artifacts with physical fallacies, degrading models into shortcut-driven “artifact detectors.” To break this bottleneck, we propose an architecture-agnostic paradigm comprising the **Programmatic Adversarial Curriculum (PACC)** and the **Visual-Anchored Reasoning Chain (VARC)**. Under a “Visually Plausible, Physically Invalid” standard, PACC systematically synthesizes multi-dimensional physical violations, decoupling artifacts from physical fallacies. Concurrently, VARC mechanistically blocks prior hijacking by compelling explicit visual grounding before physical attribution.

In summary, our main contributions are as follows: **(1) We propose the Unified Attribution Theory.** We are the first to reveal severe model fallacies in counter-intuitive scenarios and provide a unified explanation that both these and anti-physics failures fundamentally stem from semantic

priors hijacking visual evidence. **(2) We construct the Programmatic Adversarial Curriculum dataset.** It utilizes synthesized adversarial video pairs to strictly decouple generative artifacts from genuine physical fallacies for the first time. **(3) We design the Visual-Anchored Reasoning Chain to compel explicit visual grounding.** Experiments demonstrate that, without architectural overhead, standard LoRA [16] fine-tuning empowers models to break prior constraints and achieve a substantial leap in genuine physical reasoning capabilities.

2 Related Work

2.1 Physical Reasoning in Video-LLMs

Although Video-LLMs demonstrate proficiency in general understanding [21, 23, 8, 37, 46], their fine-grained physical reasoning remains limited. Interaction-heavy benchmarks [11, 15] accentuate these deficits, revealing failures in grounding physical principles like rigid-body dynamics and spatial contact. Fundamentally, these failures arise because models prioritize internal expectations over visual evidence. Existing literature typically interprets this visual neglect through multimodal hallucinations [38, 45, 30]; for instance, NOAH [17] identifies an inductive bias favoring storyline coherence, which prompts the fabrication or suppression of events to preserve narrative continuity. However, conceptualizing this visual neglect purely as a story continuation flaw overlooks the essence of physical deficits. Evaluating physical reasoning requires shifting focus from macro-level temporal coherence to immediate, low-level spatial perception. Bridging this gap, our Unified Attribution Theory reveals that physical reasoning deficits are not merely story-continuation artifacts, but stem from semantic priors acting as a severe perception bypass that overwrites explicit visual evidence.

2.2 Interventions for Physical Reasoning Deficits

Current interventions follow three primary paradigms, each with critical limitations. (1) *Architectural Modifications*: Models like TRAVL [24], PhyVLLM [42], and earlier trajectory-aware architectures [27, 6] integrate explicit trackers or Neural ODEs. Despite enhancing specific kinematics, these invasive modules incur massive computational overhead and exhibit extremely poor generalization across diverse scenarios and base models. (2) *Inference-Time Interventions*: Methods like SEASON [39] and GAVIE [22] calibrate output logits, offering only superficial patches without rectifying entrenched semantic priors within internal weights. (3) *RL Alignment*: Approaches leveraging DPO or GRPO [28, 32], including VideoHallu [20], Video-R1 [12], and VideoChat-R1 [19], suffer from severe convergence instability in high-dimensional multimodal spaces. Conversely, our Visual-Anchored Reasoning Chain (VARC) combined with standard LoRA [16] provides an architecture-agnostic, lightweight solution that mechanistically enforces visual grounding to dismantle prior interference.

2.3 Physics-Aware Video Datasets

Recent evaluation datasets [1, 24, 18] construct negative samples by capturing natural failures from text-to-video models (e.g., SVD [3], Sora [4], Kling [35], Veo [13]). However, this paradigm inherently conflates visual generative artifacts (e.g., texture flickering, object melting) with genuine physical fallacies. Consequently, evaluated models regress into shortcut-driven artifact detectors rather than rigorous physical reasoners. To overcome this, our Programmatic Adversarial Curriculum (PACC) synthesizes visually pristine yet physically invalid video pairs. By decoupling visual noise from physical logic, PACC forces models to anchor judgments on objective spatio-temporal dynamics.

3 Methodology

3.1 Overview

To resolve the reasoning failures caused by semantic prior hijacking, we propose the Programmatic Adversarial Curriculum (PACC) and the Visual-Anchored Reasoning Chain (VARC). As the data foundation, PACC dismantles the prior dominance through dual-stream paired adversarial data. Spanning eight fine-grained categories, PACC systematically generates contrastive adversarial video pairs. Each pair comprises a factual positive and a carefully manipulated negative counterpart, covering both anti-physics and counter-intuitive types. Specifically, the anti-physics stream targets

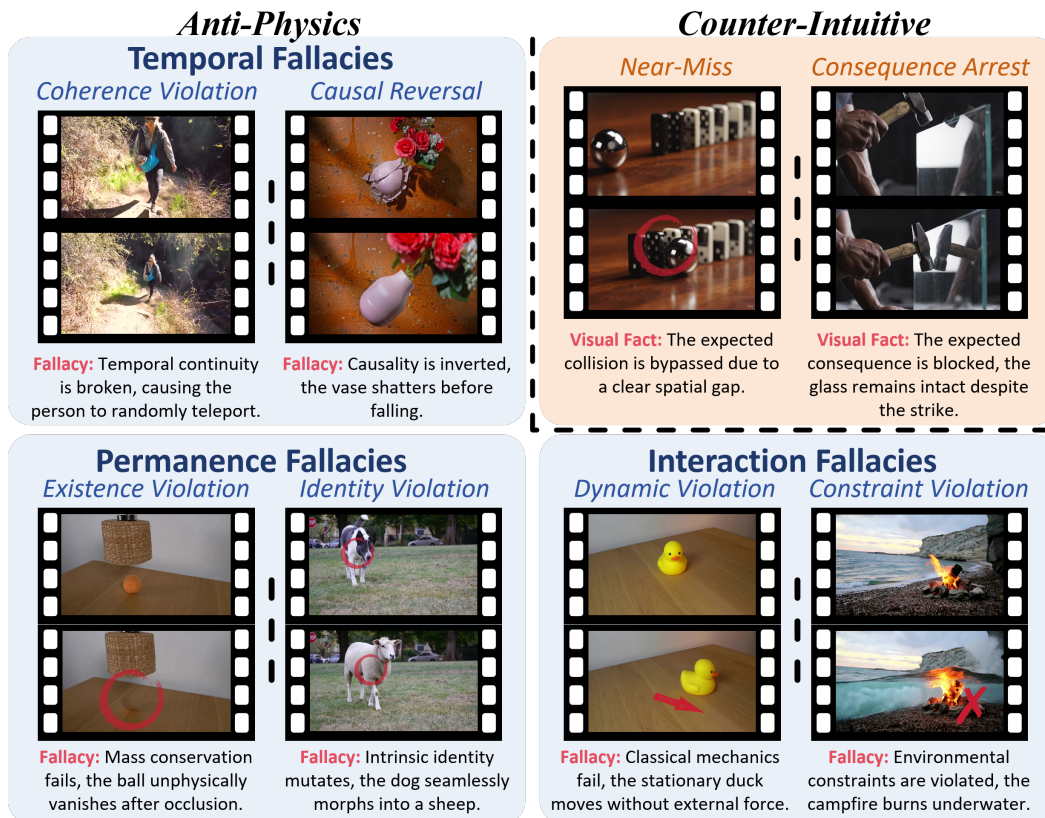


Figure 2: **Taxonomy of the PACC dataset.** The taxonomy encompasses two adversarial streams across eight fine-grained dimensions. We show only the negative counterpart of each adversarial pair, with red markers highlighting both physical violations and counter-intuitive scenarios.

rationalization fallacies: by injecting high-quality physical disruptions into the positive anchor, it forces reasoning based on objective visual evidence rather than forcefully rationalizing anomalies. The counter-intuitive stream targets stereotypical fallacies: by constructing interaction scenarios that defy expectations, it mitigates reliance on high-frequency narrative scripts. Through strictly designed physical laws and generation pipelines, PACC decouples generative artifacts from genuine physical fallacies, preventing models from exploiting them as shortcuts. Concurrently, VARC reconstructs the reasoning process into an Observation-Attribution-Verdict chain. By compelling visual fact anchoring prior to logical deduction, VARC mechanistically blocks the interference of semantic priors.

3.2 Taxonomy of PACC Adversarial Scenarios

Moving beyond the unstructured natural generative failures, PACC establishes a top-down taxonomy comprising two adversarial streams and eight fine-grained dimensions (Fig. 2). To systematically cover the fundamental limits of physical cognition rather than merely cataloging random edge cases, our categorization is deeply grounded in developmental psychology’s Core Knowledge theories [33, 2] and classic intuitive physics benchmarks [31, 41]. Specifically, the major categories map directly to the foundational principles of physical reasoning: spatio-temporal continuity (Temporal), object cohesion/permanence (Permanence), and mechanical contact (Interaction). Furthermore, instead of isolated anomalous samples, PACC constructs paired adversarial samples comprising a normal video (Positive) and its corresponding anomalous (Negative) counterpart. This paired design provides rigorous contrastive signals that force models to pinpoint explicit physical violations rather than memorizing spurious generative artifacts, and it effectively prevents models from collapsing into shortcut biases, such as defaulting to all-negative predictions. See Appendix A for more details.

Stream 1: Anti-Physics

This stream targets rationalization fallacies. Utilizing precise video editing or generative synthesis, these samples construct high-fidelity scenarios that violate objective physical laws. This forces

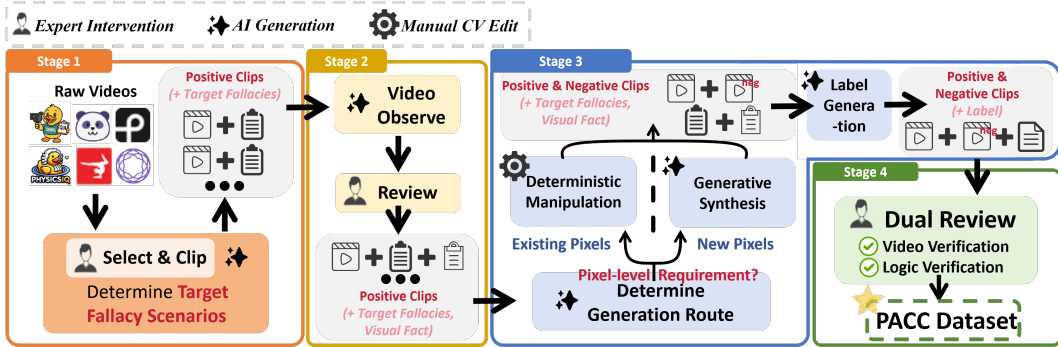


Figure 3: **The unified PACC dataset construction pipeline.** The HITL paradigm comprises four stages: (1) **Selection & Clipping** to curate positive samples with explicit physical interactions; (2) **Visual Fact Anchoring** via MLLMs and expert purification; (3) **Adversarial Generation & Label Synthesis**, which synthesizes negative counterparts via deterministic manipulation (manual CV editing) or generative synthesis (AI generation) while concurrently generating CoT labels; and (4) **Final Verification** ensuring both video and logic validity through dual expert review.

models to evaluate phenomena purely on visual facts to determine whether the video conforms to physics, rather than assuming video rationality. This stream covers three types of physical disruptions:

Temporal Fallacies (violations of time linearity and chronological causality): (1) *Coherence Violation* disrupts continuity along the micro-temporal axis (e.g., shuffling the frames of a normal walk to cause random spatial teleportation). (2) *Causal Reversal* inverts the macroscopic cause-and-effect order (e.g., a vase shattering on the ground before it is seen falling).

Permanence Fallacies (violations of mass conservation and morphological stability): (3) *Existence Violation* occurs when objects unphysically appear or disappear (e.g., a small ball abruptly vanishing after being occluded, or a massive object emerging from a tiny cover). (4) *Identity Violation* involves intrinsic properties mutating without external interaction (e.g., a dog seamlessly morphing into a sheep, or a single bouncing ball splitting into multiple).

Interaction Fallacies (violations of causal consistency): (5) *Dynamic Violation* deviates from classical mechanics and thermodynamics. This encompasses Newtonian motion failures (e.g., a toy duck moving without external force, or moving objects instantly freezing), force equilibrium violations (e.g., the heavier end of a seesaw remaining suspended, or unsupported blocks defying gravity), and entropy reversals (e.g., shattered objects spontaneously reassembling). (6) *Constraint Violation* encompasses causal imbalances or rigid-body failures (e.g., a fire burning underwater, a small stone splashing a massive wave, or solid objects passing directly through each other).

Stream 2: Counter-Intuitive

This stream targets stereotypical fallacies. These samples are physically plausible but construct adversarial states where expected events fail to occur. They penalize models for ignoring clear visual evidence and blindly hallucinating outcomes based on statistical priors. (7) *Near-Miss*: The trajectory enters an interaction zone, but the spatial gap does not lead to contact (e.g., a ball brushing past dominoes without touching, or a foot missing a football). This forces the model to verify objective visual states rather than directly predicting an inevitable collision. (8) *Consequence Arrest*: The initial action is established, but the expected consequence is blocked by insufficient force or hidden factors (e.g., a hammer striking glass but failing to break it, or a tilted cup not spilling its liquid).

3.3 The Unified PACC Pipeline

PACC adopts a rigorous **Human-in-the-loop (HITL)** collaborative construction paradigm, integrating video generation models with precise manual intervention to guarantee both adversarial diversity and physical rigor. Raw materials are curated from established datasets (e.g., Something-Something V2 [14], PhysBench [11], Panda-70M [7], ImplausiBench [24], ActivityNet [5], Physics-IQ [25]) and royalty-free platforms (e.g., Pexels¹). The pipeline consists of four stages (Fig. 3):

¹<https://www.pexels.com/>

Stage 1: Selection & Clipping. Experts manually screen high-quality source videos exhibiting a singular physical interaction. With LLM assistance, these videos are mapped to target taxonomic dimensions and annotated with corresponding target fallacy scenarios. By trimming redundant frames, we isolate atomic slices of core physical interactions. These constitute the initial *positive samples*.

Stage 2: Visual Fact Anchoring. Multimodal LLMs (e.g., Gemini 3.1 Preview) generate purely observational captions for the positive samples. Experts subsequently perform rigorous cleaning to: (1) ensure *purity* by eliminating visual hallucinations; and (2) maintain *objectivity* by strictly prohibiting physical speculation (e.g., “falling due to gravity”). This yields purely visual fact anchors.

Stage 3: Adversarial Generation & Label Synthesis. Based on the positive video, visual facts, and target fallacy, the pipeline routes and synthesizes *negative samples* to form adversarial pairs. Driven by pixel-level requirements, this process bifurcates into two paths: **(1) Deterministic Manipulation:** For fallacies requiring the rearrangement of existing pixels or temporal manipulation (e.g., frame shuffling, mask-based erasure), experts perform manual editing utilizing models like SAM2 [29] and ProPainter [47]. **(2) Generative Synthesis:** For fallacies requiring the synthesis of new pixels or alteration of physical properties (e.g., morphological mutation, trajectory deviation), we deploy prompt-driven video generation models (e.g., Kling). Concurrently, the LLM synthesizes the paired Chain-of-Thought (CoT) labels, comprising Observation, Attribution, and Verdict (Sec. 3.4).

Stage 4: Final Verification. All entries undergo dual expert review. **Video Verification** ensures the negative sample constitutes an unambiguous physical fallacy, discarding visually plausible generative failures. **Logic Verification** scrutinizes the scientific accuracy of the label’s attribution logic.

Dataset Statistics and Properties. Through the rigorous HITL construction pipeline, the PACC dataset yields **758** high-fidelity adversarial video pairs (**1,516** independent clips). The average video duration is **4.0** seconds, strictly focusing on a singular physical interaction. The adversarial pairs are distributed across the eight fallacy dimensions: Coherence Violation (**11.1%**), Causal Reversal (**11.1%**), Existence Violation (**5.4%**), Identity Violation (**6.1%**), Dynamic Violation (**27.1%**), Constraint Violation (**19.0%**), Near-Miss (**14.1%**), and Consequence Arrest (**6.1%**). While PACC prioritizes ultra-high fidelity and rigorous expert verification over sheer volume, our standardized construction pipeline ensures that the dataset can be seamlessly scaled in future iterations.

3.4 Visual-Anchored Reasoning Chain (VARC)

To mitigate the semantic inertia where models prioritize linguistic priors over visual evidence, we propose the Visual-Anchored Reasoning Chain (VARC). Traditional Video-LLMs estimate the verdict probability $P(y|V, Q)$ given video V and query Q . However, dominated by semantic priors, this estimation frequently degenerates into a visual-agnostic shortcut $P(y|Q)$. To sever this shortcut, VARC formulates the reasoning process as a directed Markovian chain, incorporating the intermediate visual observation O and the model’s built-in physical knowledge base \mathcal{K} . We assume the conditional independence of downstream logical judgments once explicit visual evidence is extracted:

$$P(y|V, Q) \approx P(O|V) \cdot P(A|O, \mathcal{K}) \cdot P(y|O, A). \quad (1)$$

Step 1: Forced Observation ($\sim P(O|V)$). This step compels the model to ground its reasoning purely on visual evidence, explicitly blocking hallucinations driven by semantic completion. The model must describe low-level spatial relationships and state changes (e.g., specifying a “spatial gap”) without premature subjective judgment.

Step 2: Causal Attribution ($\sim P(A|O, \mathcal{K})$). Conditioned on the objective observation O , the model queries its physical knowledge \mathcal{K} to provide causal attribution. Instead of hallucinating hidden variables to rationalize anomalies, it utilizes the logical conflict between O and \mathcal{K} to detect physical fallacies (e.g., recognizing the thermodynamic impossibility of a fire burning underwater).

Step 3: Evidence-Based Verdict ($\sim P(y|O, A)$). The final verdict y is strictly constrained by the preceding observation and attribution nodes. VARC transforms the implicitly vulnerable judgment process into a rigorous causal verification firmly anchored in visual facts.

3.5 Adversarial Curriculum and Paired Gradient Suppression

To mitigate shortcut learning on shallow visual features during Supervised Fine-Tuning (SFT), we introduce an adversarial curriculum based on paired data binding. Specifically, aligned positive

Table 1: **Pair-wise Consistency Accuracy (PCA) on the PACC test set.** The eight sub-categories are grouped by stream. *Anti-physics*: Coh. (Coherence), Cau. (Causal Reversal), Exi. (Existence), Ide. (Identity), Dyn. (Dynamic), and Cns. (Constraint). *Counter-intuitive*: N-Miss (Near Miss) and C-Arrest (Consequence Arrest). Best and second-best results are **bolded** and underlined.

Method	Anti-Physics						Counter-Intuitive		Avg.↑
	Coh.	Cau.	Exi.	Ide.	Dyn.	Cns.	N-Miss	C-Arrest	
<i>Proprietary Models</i>									
GPT-4o	43.80	<u>41.20</u>	55.60	50.00	<u>35.70</u>	<u>21.40</u>	<u>45.50</u>	<u>40.00</u>	38.31
Gemini 2.5 Flash	56.20	52.90	55.60	40.00	45.20	25.00	27.20	<u>40.00</u>	<u>40.91</u>
<i>Open-Source Models</i>									
Flash-VStream-7B	0.00	0.00	0.00	0.00	0.00	0.00	4.50	0.00	0.65
Video-ChatGPT-7B	0.00	5.90	0.00	0.00	0.00	0.00	0.00	0.00	0.65
InternVL2.5-8B	0.00	5.90	0.00	10.00	4.80	0.00	0.00	0.00	2.60
Video-LLaVA-7B	0.00	0.00	0.00	0.00	4.80	7.10	0.00	0.00	2.60
MiniCPM-V 2.6	0.00	5.90	0.00	10.00	4.80	3.60	4.50	0.00	3.90
VideoLLaMA2-7B	0.00	5.90	0.00	10.00	11.90	3.60	4.50	0.00	5.84
VideoLLaMA3-7B	0.00	5.90	0.00	10.00	14.30	3.60	9.10	10.00	7.79
Qwen3.5-35B	6.20	17.60	11.10	30.00	16.70	10.70	9.10	10.00	13.64
Ours (PhyAR)	<u>50.00</u>	52.90	<u>22.20</u>	50.00	28.60	<u>21.40</u>	68.20	70.00	41.56

and negative video pairs are jointly optimized. During training, sampling is randomized across pairs (*inter-pair*), while the sequence within each pair (*intra-pair*) remains bound. This paired backpropagation induces *Gradient Suppression*: gradients derived from shared visual semantics (e.g., backgrounds, lighting, static object appearance) are mitigated. Consequently, the optimization naturally bypasses static visual distributions, converging strictly on the core physical discrepancy.

Since pilot studies confirm intact low-level perception, we freeze the vision encoder and apply LoRA [16] exclusively to the visual projector and LLM backbone, strictly targeting the reasoning bottleneck. This yields **PhyAR (Physics-Anchored Reasoner)**. Through this targeted update, PhyAR performs physical reasoning based on visual perception without extensive structural modifications.

4 Experiments

4.1 Experimental Setup

Baselines. We evaluate PhyAR against SOTA Video-LLMs, including open-source models (Qwen3.5-35B [36], InternVL2.5-8B [9], MiniCPM-V 2.6 [40], VideoLLaMA2-7B [10], VideoLLaMA3-7B [43], Video-LLaVA-7B [21], Flash-VStream-7B [44], and Video-ChatGPT-7B [23]) and proprietary models (Gemini 2.5 Flash [34] and GPT-4o [26]). All experiments are conducted on the PACC test set (154 video pairs, 308 videos). All models uniformly sample 16 frames per video, and open-source models are deployed in 16-bit precision.

Evaluation Metrics. We use **Pair-wise Consistency Accuracy (PCA)** as the primary metric to evaluate the dual-stream PACC dataset, with specific criteria: (1) **Anti-physics Stream**: Models must correctly identify whether the video violates physical laws. (2) **Counter-intuitive Stream**: Models must accurately describe the objective video phenomena without succumbing to intuitive priors. Crucially, a pair is deemed correct only if the model succeeds on *both* the positive and negative samples. To evaluate logical reasoning quality, we employ an LLM-as-a-Judge (Gemini 2.5 Pro) [23] to compute the **Reasoning Alignment Score (RAS)** (scaled 1-5), measuring rigorous alignment between the model’s textual explanations and the visual ground truth.

Implementation. PhyAR builds upon VideoLLaMA3-7B [43]. It is fine-tuned on the PACC training set (604 video pairs, 1,208 videos) for 3 epochs using LoRA (see Appendix B). We apply paired data binding to induce gradient suppression (Sec. 3.5). All models use the standardized VARC prompt for formatting consistency. Baselines are evaluated zero-shot using official pre-trained weights.

Table 2: **Reasoning Alignment Score (RAS) (scaled 1-5) on the PACC test set.** Sub-category abbreviations and highlighting conventions follow Table 1.

Method	Anti-Physics						Counter-Intuitive		Avg.↑
	Coh.	Cau.	Exi.	Ide.	Dyn.	Cns.	N-Miss	C-Arrest	
<i>Proprietary Models</i>									
GPT-4o	2.156	2.324	2.667	2.500	2.048	1.679	2.250	2.100	2.120
Gemini 2.5 Flash	2.469	2.441	2.833	<u>2.300</u>	2.571	1.875	1.818	<u>2.200</u>	2.286
<i>Open-Source Models</i>									
Flash-VStream-7B	1.125	1.176	1.222	1.000	1.024	1.107	1.182	1.050	1.101
Video-ChatGPT-7B	1.000	1.206	1.056	1.100	1.048	1.089	1.045	1.100	1.075
InternVL2.5-8B	1.000	1.147	1.000	1.300	1.131	1.143	1.091	1.100	1.117
Video-LLaVA-7B	1.000	1.000	1.000	1.000	1.095	1.143	1.136	1.150	1.081
MiniCPM-V 2.6	1.125	1.118	1.333	1.450	1.167	1.161	1.159	1.150	1.182
VideoLLaMA2-7B	1.000	1.118	1.111	1.250	1.238	1.071	1.204	1.250	1.159
VideoLLaMA3-7B	1.000	1.118	1.222	1.200	1.262	1.268	1.386	1.350	1.237
Qwen3.5-35B	1.125	1.529	1.500	1.950	1.524	1.429	1.409	1.550	1.477
Ours (PhyAR)	<u>2.375</u>	2.294	1.611	2.050	1.619	<u>1.732</u>	2.523	2.950	2.036

4.2 Main Results

Comparative results on Pair-wise Consistency Accuracy (PCA). Table 1 compares our proposed framework against SOTA Video-LLMs, demonstrating that PhyAR achieves the best overall performance with an average PCA of 41.56%. Driven by the explicit visual grounding of VARC, our model exhibits a remarkable performance leap in the Counter-intuitive stream, effectively mitigating severe semantic inertia. While massive proprietary models (e.g., GPT-4o) retain localized advantages in specific Anti-physics tasks (e.g., Dynamic Violation) leveraging their extensive pre-trained world knowledge, PhyAR secures substantial global gains across the benchmark. This effectiveness is attributed to the synergy of VARC and paired optimization, which prevents the model from defaulting to data priors and explicitly dismantles the ubiquitous *Yes-bias* plaguing baseline models. Specifically, smaller open-source models systematically collapse to semantic priors, predicting affirmative outcomes by default (i.e., assuming all videos are physically plausible). Consequently, they consistently fail on the negative counterparts, leading to their degraded PCA scores.

Comparative results on Reasoning Alignment Score (RAS). As shown in Table 2, proprietary models (GPT-4o and Gemini 2.5 Flash) lead in RAS. This advantage stems from their massive scale and extensive world knowledge, facilitating detailed textual attributions for physical phenomena. However, whereas most open-source baselines stagnate near the 1.0 lower bound, our PhyAR achieves a substantial improvement (average score of 2.036). Crucially, in the Counter-Intuitive categories which demand strict adherence to visual facts, PhyAR surpasses all baselines. This finding underscores a fundamental bottleneck in multimodal physical reasoning: massive models are heavily constrained by semantic inertia, frequently bypassing fine-grained visual observation to output conclusions dictated by data priors. Conversely, by enforcing visual grounding via VARC, PhyAR demonstrates that valid physical deduction must be anchored in objective observation, and generative capabilities alone cannot compensate for factual blindness in counter-intuitive scenarios.

4.3 Ablation Study

Table 3 details the ablation of VARC and pair-wise optimization on the PACC test set.

Ablation of VARC. Removing the VARC mechanism decreases the average Pair-wise Consistency Accuracy (PCA) from 41.56% to 28.57%. This performance drop confirms that without explicit visual grounding, the model collapses to semantic priors. Consequently, it bypasses actual visual observation, failing to ground its reasoning in the objective physical facts present in the video.

Ablation of Pair-wise Optimization. Omitting pair-wise optimization drops the PCA to 29.22%. This validates that paired gradient suppression effectively dismantles the inherent Yes-bias of the baseline, which enables the model to learn the core physical discrepancies between positive and negative samples, accurately identifying physical violations within adversarial pairs.

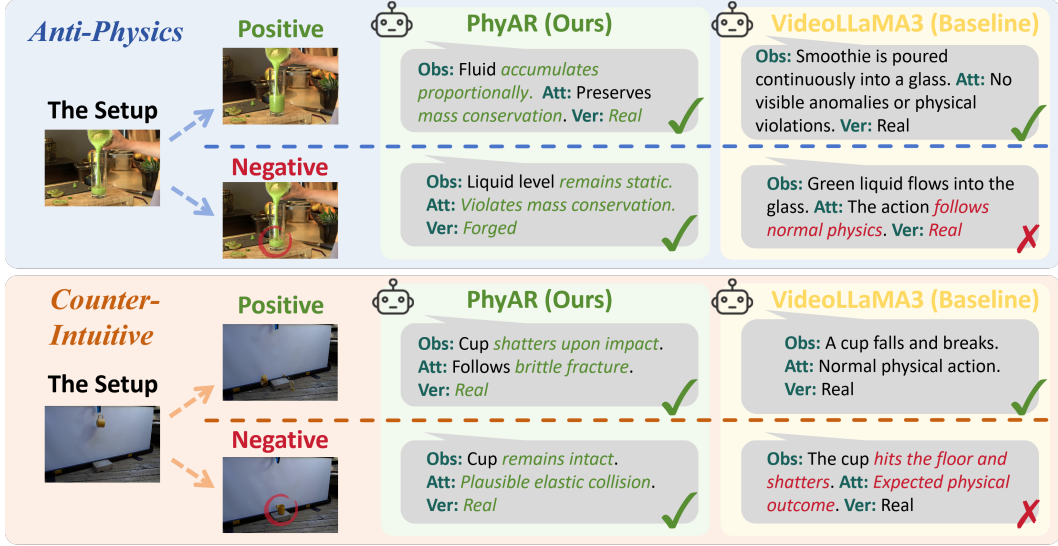


Figure 4: **Qualitative comparison on the PACC dataset.** The baseline fails to detect the physical violation (top) and hallucinates an expected outcome (bottom). PhyAR consistently anchors its reasoning on objective visual facts.

Table 3: **Ablation study of the VARC mechanism and pair-wise optimization.** Evaluated on the PACC test set.

Method	PCA Avg. (↑)	RAS Avg. (↑)
Baseline SFT	24.68	1.760
w/o VARC	28.57	1.802
w/o Pair-wise	29.22	1.763
PhyAR (Full)	41.56	2.036

Table 4: **Quantitative analysis of semantic prior bias using the RPB metric.** PhyAR significantly suppresses prior dependence while improving overall point-wise accuracy.

Metric	VideoLLaMA3 (Base)	PhyAR (Ours)
Acc_{pos} (%)	93.1	79.9
Acc_{neg} (%)	10.8	48.1
Overall Acc (%) (↑)	51.9	64.0
RPB (%) (↓)	79.1	24.9

Ultimately, these results demonstrate that both components are essential for the model to overcome semantic priors and anchor its reasoning on visual facts.

4.4 Analysis on Semantic Prior Bias

To quantitatively assess the model’s vulnerability to semantic priors, we introduce the Relative Prior Bias (RPB). Inspired by the Michelson contrast, RPB measures the dominance of semantic priors over objective visual evidence by comparing point-wise accuracy on prior-aligned positive (Acc_{pos}) and prior-violating negative (Acc_{neg}) samples:

$$RPB = \frac{Acc_{pos} - Acc_{neg}}{Acc_{pos} + Acc_{neg}}. \quad (2)$$

As detailed in Table 4, the base model (VideoLLaMA3) exhibits a severe RPB of 79.1%. The stark disparity between its performance on positive (93.1%) and negative (10.8%) samples reveals its decision process is heavily dictated by data priors. When encountering familiar physical concepts, the model defaults to affirmative predictions, ignoring contradictory visual facts. In contrast, PhyAR overcomes this prior reliance, reducing the RPB to 24.9% while improving overall accuracy to 64.0%.

4.5 Qualitative Analysis

Figure 4 visualizes the qualitative comparison on two adversarial pairs from the PACC dataset.

In the **Anti-Physics** scenario (top), a continuous stream of liquid anomalously fails to accumulate in the glass. The baseline model entirely misses this glaring physical anomaly and blindly predicts

“Real”. Conversely, PhyAR correctly grounds its observation on the static liquid level and attributes it to a conservation violation.

In the **Counter-Intuitive** scenario (bottom), a dropped cup unexpectedly remains intact. The baseline model exhibits severe visual hallucination, fabricating a non-existent “shattering” event to fit its statistical expectation. PhyAR successfully resists this prior trap, anchoring its judgment on the intact cup and accurately identifying a plausible elastic collision. These results confirm that PhyAR effectively neutralizes semantic prior hijacking via visual grounding.

Conclusion and Limitations. We propose the Unified Attribution Theory and PACC to resolve Semantic Prior Dominance in Video-LLMs via VARC and adversarial curriculum, yielding substantial physical reasoning gains. Although PACC is currently limited to 758 rigorously verified pairs due to strict human-in-the-loop expert validation, this design intentionally prioritizes high fidelity and physical rigor over sheer scale, making it a precise diagnostic benchmark akin to CLEVRER[41] and IntPhys[31]. Future work will explore automated synthesis for broader scaling while preserving annotation quality.

References

- [1] Zechen Bai, Hai Ci, and Mike Zheng Shou. Impossible videos. In *International Conference on Machine Learning*, 2025.
- [2] Renée Baillargeon. The acquisition of physical knowledge in infancy: A summary in eight lessons. In *Blackwell handbook of childhood cognitive development*, pages 47–83. Wiley Online Library, 2002.
- [3] Andreas Blattmann, Tim Dockhorn, Sumith Kulal, Daniel Mendelevitch, Maciej Kilian, Dominik Lorenz, Yam Levi, Zion English, Vikram Voleti, Adam Letts, et al. Stable video diffusion: Scaling latent video diffusion models to large datasets. *arXiv preprint arXiv:2311.15127*, 2023.
- [4] Tim Brooks, Bill Peebles, Connor Holmes, Will DePue, Yufei Guo, Leo Jing, David Schnurr, Joe Taylor, Troy Luhman, Eric Luhman, et al. Video generation models as world simulators. <https://openai.com/research/video-generation-models-as-world-simulators>, 2024.
- [5] Fabian Caba Heilbron, Victor Escorcia, Bernard Ghanem, and Juan Carlos Niebles. Activitynet: A large-scale video benchmark for human activity understanding. In *Proceedings of the IEEE conference on computer vision and pattern recognition*, pages 961–970, 2015.
- [6] Hila Chefer, Uriel Singer, Amit Zohar, Yuval Kirstain, Adam Polyak, Yaniv Taigman, Lior Wolf, and Shelly Sheynin. Videojam: Joint appearance-motion representations for enhanced motion generation in video models. *arXiv preprint arXiv:2502.02492*, 2025.
- [7] Tsai-Shien Chen, Aliaksandr Siarohin, Willi Menapace, Ekaterina Deyneka, Hsiang-wei Chao, Byung Eun Jeon, Yuwei Fang, Hsin-Ying Lee, Jian Ren, Ming-Hsuan Yang, et al. Panda-70m: Captioning 70m videos with multiple cross-modality teachers. In *Proceedings of the IEEE/CVF Conference on Computer Vision and Pattern Recognition*, pages 13320–13331, 2024.
- [8] Yukang Chen, Fuzhao Xue, Dacheng Li, Qinghao Hu, Ligeng Zhu, Xiuyu Li, Yunhao Fang, Haotian Tang, Shang Yang, Zhijian Liu, et al. Longvila: Scaling long-context visual language models for long videos. In *International Conference on Learning Representations*, 2025.
- [9] Zhe Chen, Weiyun Wang, Yue Cao, Yangzhou Liu, Zhangwei Gao, Erfei Cui, Jinguo Zhu, Shenglong Ye, Hao Tian, Zhaoyang Liu, et al. Expanding performance boundaries of open-source multimodal models with model, data, and test-time scaling. *arXiv preprint arXiv:2412.05271*, 2024.
- [10] Zesen Cheng, Sicong Leng, Hang Zhang, Yifei Xin, Xin Li, Guanzheng Chen, Yongxin Zhu, Wenqi Zhang, Ziyang Luo, Deli Zhao, et al. Videollama 2: Advancing spatial-temporal modeling and audio understanding in video-llms. *arXiv preprint arXiv:2406.07476*, 2024.
- [11] Wei Chow, Jiageng Mao, Boyi Li, Daniel Seita, Vitor Guizilini, and Yue Wang. Physbench: Benchmarking and enhancing vision-language models for physical world understanding. *arXiv preprint arXiv:2501.16411*, 2025.

- [12] Kaituo Feng, Kaixiong Gong, Bohao Li, Zonghao Guo, Yibing Wang, Tianshuo Peng, Junfei Wu, Xiaoying Zhang, Benyou Wang, and Xiangyu Yue. Video-r1: Reinforcing video reasoning in mllms. *arXiv preprint arXiv:2503.21776*, 2025.
- [13] Google DeepMind. Veo: A text-to-video generation system. Technical report, Google, 2025. URL <https://storage.googleapis.com/deepmind-media/veo/Veo-3-Tech-Report.pdf>.
- [14] Raghav Goyal, Samira Ebrahimi Kahou, Vincent Michalski, Joanna Materzynska, Susanne Westphal, Heuna Kim, Valentin Haenel, Ingo Fruend, Peter Yianilos, Moritz Mueller-Freitag, et al. The "something something" video database for learning and evaluating visual common sense. In *Proceedings of the IEEE international conference on computer vision*, pages 5842–5850, 2017.
- [15] Wenyi Hong, Yean Cheng, Zhuoyi Yang, Weihang Wang, Lefan Wang, Xiaotao Gu, Shiyu Huang, Yuxiao Dong, and Jie Tang. Motionbench: Benchmarking and improving fine-grained video motion understanding for vision language models. In *Proceedings of the Computer Vision and Pattern Recognition Conference*, pages 8450–8460, 2025.
- [16] Edward J Hu, Yelong Shen, Phil Wallis, Zeyuan Allen-Zhu, Yuanzhi Li, Shean Wang, Lu Wang, and Weizhu Chen. Lora: Low-rank adaptation of large language models. In *International Conference on Learning Representations*, 2022.
- [17] Kyuho Lee, Euntae Kim, Jinwoo Choi, and Buru Chang. Noah: Benchmarking narrative prior driven hallucination and omission in video large language models. *arXiv preprint arXiv:2511.06475*, 2025.
- [18] Dacheng Li, Yunhao Fang, Yukang Chen, Shuo Yang, Shiyi Cao, Justin Wong, Michael Luo, Xiaolong Wang, Hongxu Yin, Joseph E Gonzalez, et al. Worldmodelbench: Judging video generation models as world models. *arXiv preprint arXiv:2502.20694*, 2025.
- [19] Xinhao Li, Ziang Yan, Desen Meng, Lu Dong, Xiangyu Zeng, Yinan He, Yali Wang, Yu Qiao, Yi Wang, and Limin Wang. Videochat-r1: Enhancing spatio-temporal perception via reinforcement fine-tuning. *arXiv preprint arXiv:2504.06958*, 2025.
- [20] Zongxia Li, Xiyang Wu, Guangyao Shi, Yubin Qin, Hongyang Du, Fuxiao Liu, Tianyi Zhou, Dinesh Manocha, and Jordan Lee Boyd-Graber. Videohallu: Evaluating and mitigating multi-modal hallucinations on synthetic video understanding. *arXiv preprint arXiv:2505.01481*, 2025.
- [21] Bin Lin, Yang Ye, Bin Zhu, Jiayi Cui, Munan Ning, Peng Jin, and Li Yuan. Video-llava: Learning united visual representation by alignment before projection. In *Proceedings of the 2024 conference on empirical methods in natural language processing*, pages 5971–5984, 2024.
- [22] Fuxiao Liu, Kevin Lin, Linjie Li, Jianfeng Wang, Yaser Yacoob, and Lijuan Wang. Mitigating hallucination in large multi-modal models via robust instruction tuning. In B. Kim, Y. Yue, S. Chaudhuri, K. Fragkiadaki, M. Khan, and Y. Sun, editors, *International Conference on Learning Representations*, volume 2024, pages 57689–57733, 2024. URL https://proceedings.iclr.cc/paper_files/paper/2024/file/fed9263d7f1086e735904ff690527a53-Paper-Conference.pdf.
- [23] Muhammad Maaz, Hanoona Rasheed, Salman Khan, and Fahad Khan. Video-chatgpt: Towards detailed video understanding via large vision and language models. In *Proceedings of the 62nd Annual Meeting of the Association for Computational Linguistics (Volume 1: Long Papers)*, pages 12585–12602, 2024.
- [24] Saman Motamed, Minghao Chen, Luc Van Gool, and Iro Laina. Travl: A recipe for making video-language models better judges of physics implausibility. *arXiv preprint arXiv:2510.07550*, 2025.
- [25] Saman Motamed, Laura Culp, Kevin Swersky, Priyank Jaini, and Robert Geirhos. Do generative video models understand physical principles? In *Proceedings of the IEEE/CVF Winter Conference on Applications of Computer Vision*, pages 948–958, 2026.

- [26] OpenAI. GPT-4o technical report. Technical report, OpenAI, 2024. URL <https://openai.com/index/hello-gpt-4o/>.
- [27] Mandela Patrick, Dylan Campbell, Yuki Asano, Ishan Misra, Florian Metze, Christoph Feichtenhofer, Andrea Vedaldi, and Joao F Henriques. Keeping your eye on the ball: Trajectory attention in video transformers. In *Advances in Neural Information Processing Systems*, volume 34, pages 12493–12506, 2021.
- [28] Rafael Rafailov, Archit Sharma, Eric Mitchell, Christopher D Manning, Stefano Ermon, and Chelsea Finn. Direct preference optimization: Your language model is secretly a reward model. In *Advances in Neural Information Processing Systems*, volume 36, pages 53728–53741, 2023.
- [29] Nikhila Ravi, Valentin Gabeur, Yuan-Ting Hu, Ronghang Hu, Chaitanya Ryali, Tengyu Ma, Haitham Khedr, Roman Rädle, Chloe Rolland, Laura Gustafson, et al. Sam 2: Segment anything in images and videos. *arXiv preprint arXiv:2408.00714*, 2024.
- [30] Ruchit Rawal, Reza Shirkavand, Heng Huang, Gowthami Somepalli, and Tom Goldstein. Argus: Hallucination and omission evaluation in video-llms. In *Proceedings of the IEEE/CVF International Conference on Computer Vision*, pages 20280–20290, 2025.
- [31] Ronan Riochet, Mario Ynocente Castro, Mathieu Bernard, Adam Lerer, Rob Fergus, Véronique Izard, and Emmanuel Dupoux. Intphys: A framework and benchmark for visual intuitive physics reasoning. *arXiv preprint arXiv:1803.07616*, 2018.
- [32] Zhihong Shao, Peiyi Wang, Qihao Zhu, Runxin Xu, Junxiao Song, Xiao Bi, Haowei Zhang, Mingchuan Zhang, YK Li, Yang Wu, et al. Deepseekmath: Pushing the limits of mathematical reasoning in open language models. *arXiv preprint arXiv:2402.03300*, 2024.
- [33] Elizabeth S Spelke. Principles of object perception. *Cognitive science*, 14(1):29–56, 1990.
- [34] Gemini Team, Petko Georgiev, Ving Ian Lei, Ryan Burnell, Libin Bai, Anmol Gulati, Garrett Tanzer, Damien Vincent, Zhufeng Pan, Shibo Wang, et al. Gemini 1.5: Unlocking multimodal understanding across millions of tokens of context. *arXiv preprint arXiv:2403.05530*, 2024.
- [35] Kling Team, Jialu Chen, Yuanzheng Ci, Xiangyu Du, Zipeng Feng, Kun Gai, Sainan Guo, Feng Han, Jingbin He, Kang He, et al. Kling-omni technical report. *arXiv preprint arXiv:2512.16776*, 2025.
- [36] Qwen Team. Qwen 3.5 technical report. <https://qwen.ai/blog?id=qwen3.5>, 2026.
- [37] Yi Wang, Xinhao Li, Ziang Yan, Yinan He, Jiashuo Yu, Xiangyu Zeng, Chenting Wang, Changlian Ma, Haiyan Huang, Jianfei Gao, et al. Internvideo2. 5: Empowering video mllms with long and rich context modeling. *arXiv preprint arXiv:2501.12386*, 2025.
- [38] Yuxuan Wang, Yueqian Wang, Dongyan Zhao, Cihang Xie, and Zilong Zheng. Videohalluc: Evaluating intrinsic and extrinsic hallucinations in large video-language models. *arXiv preprint arXiv:2406.16338*, 2024.
- [39] Chang-Hsun Wu, Kai-Po Chang, Yu-Yang Sheng, Hung-Kai Chung, Kuei-Chun Wang, and Yu-Chiang Frank Wang. Season: Mitigating temporal hallucination in video large language models via self-diagnostic contrastive decoding. *arXiv preprint arXiv:2512.04643*, 2025.
- [40] Yuan Yao, Tianyu Yu, Ao Zhang, Chongyi Wang, Junbo Cui, Hongji Zhu, Tianchi Cai, Haoyu Li, Weilin Zhao, Zhihui He, et al. Minicpm-v: A gpt-4v level mllm on your phone. *arXiv preprint arXiv:2408.01800*, 2024.
- [41] Kexin Yi, Chuang Gan, Yunzhu Li, Pushmeet Kohli, Jiajun Wu, Antonio Torralba, and Joshua B Tenenbaum. Clevrer: Collision events for video representation and reasoning. In *International Conference on Learning Representations*, 2020.
- [42] Yu-Wei Zhan, Xin Wang, Hong Chen, Tongtong Feng, Wei Feng, Ren Wang, Guangyao Li, Qing Li, and Wenwu Zhu. Phyvllm: Physics-guided video language model with motion-appearance disentanglement. *arXiv preprint arXiv:2512.04532*, 2025.

- [43] Boqiang Zhang, Kehan Li, Zesen Cheng, Zhiqiang Hu, Yuqian Yuan, Guanzheng Chen, Sicong Leng, Yuming Jiang, Hang Zhang, Xin Li, et al. Videollama 3: Frontier multimodal foundation models for image and video understanding. *arXiv preprint arXiv:2501.13106*, 2025.
- [44] Haoji Zhang, Yiqin Wang, Yansong Tang, Yong Liu, Jiashi Feng, Jifeng Dai, and Xiaojie Jin. Flash-vstream: Memory-based real-time understanding for long video streams. *arXiv preprint arXiv:2406.08085*, 2024.
- [45] Jiacheng Zhang, Yang Jiao, Shaoxiang Chen, Na Zhao, Zhiyu Tan, Hao Li, Xingjun Ma, and Jingjing Chen. Eventhallusion: Diagnosing event hallucinations in video llms. *arXiv preprint arXiv:2409.16597*, 2024.
- [46] Zicheng Zhao, Kangyu Wang, Shijie Li, Rui Qian, Weiyao Lin, and Huabin Liu. Cogstream: Context-guided streaming video question answering. In *Proceedings of the AAAI Conference on Artificial Intelligence*, volume 40, pages 13332–13341, 2026.
- [47] Shangchen Zhou, Chongyi Li, Kelvin CK Chan, and Chen Change Loy. Propainter: Improving propagation and transformer for video inpainting. In *Proceedings of the IEEE/CVF international conference on computer vision*, pages 10477–10486, 2023.
- [48] Brianna Zitkovich, Tianhe Yu, Sichun Xu, Peng Xu, Ted Xiao, Fei Xia, Jialin Wu, Paul Wohlhart, Stefan Welker, Ayzaan Wahid, et al. Rt-2: Vision-language-action models transfer web knowledge to robotic control. In *Conference on Robot Learning*, pages 2165–2183. PMLR, 2023.

A Detailed Taxonomy and Qualitative Examples of PACC

Building upon the taxonomy introduced in Section 3.2, this appendix provides a comprehensive breakdown of the Programmatic Adversarial Curriculum (PACC) dataset. For every adversarial pair in PACC, we synthesize detailed Chain-of-Thought (CoT) annotations, encompassing an objective visual observation, an attribution of the physical logic (valid or invalid), and a final verdict. The dataset is strictly organized into two adversarial streams across eight fine-grained dimensions.

In addition, the supplementary material contains eight representative case studies. These examples serve as concrete illustrations of the PACC construction pipeline and labeling standards across all eight dimensions.

A.1 Stream 1: Anti-Physics

This stream targets rationalization fallacies by violating objective physical laws.

Temporal Fallacies

Core Principle: Violations of time linearity and chronological causality.

(1) Coherence Violation

- **Definition:** Disrupts the micro-temporal continuity of actions.
- **Examples:** A video of a car driving continuously along a straight road is temporally shuffled, causing the car to randomly teleport back and forth to different positions.

(2) Causal Reversal

- **Definition:** Inverts the macroscopic logical order of cause and effect (the consequence precedes the cause).
- **Examples:** A video is temporally edited so that a glass shatters on the floor (effect) before the person is seen throwing it (cause).

Permanence Fallacies

Core Principle: Violations of mass conservation and morphological stability. Objects must remain consistent unless explicitly interacted with.

(3) Existence Violation

- **Definition:** Unphysical appearance or disappearance of objects in space-time.
- **Examples:**
 - An object vanishes or materializes out of thin air in an unoccluded close-up shot (e.g., an object resting on a table suddenly disappears; pouring “empty air” into a cup, yet the liquid level continuously rises).
 - An object physically disappears after being covered (e.g., a cloth is placed over an object, but the cloth collapses completely flat).
 - An object vanishes into thin air after being covered and subsequently uncovered.
 - An object physically appears after removing a cover (e.g., removing a small cloth reveals a massive object that could not possibly be concealed beneath it).

(4) Identity Violation

- **Definition:** Intrinsic properties of an object mutate abruptly without corresponding external interaction.
- **Examples:** (*Quantity*) A single bouncing ball spontaneously splits into multiple balls upon hitting the ground; (*Morphology*) A quail seamlessly morphs into a rooster mid-walk.

Interaction Fallacies

Core Principle: Violations of causal consistency in physical interactions.

(5) Dynamic Violation

- **Definition:** Violates kinematics (Newton's laws of motion), mechanical equilibrium, or the thermodynamic arrow of time (entropy).
- **Examples:**
 - *Newton's First Law / Momentum Loss:* An object sliding on a frictionless surface (e.g., curling stone, billiard ball) instantaneously freezes without gradual deceleration; an object hits an "invisible wall" and suddenly stops or bounces back; an object pushed onto a high-friction surface (e.g., carpet) accelerates instead of decelerating, or slides off the screen at a constant speed (ignoring friction); a high-speed ball A strikes a stationary ball B, yet both instantly stop upon impact (momentum vanishes); a bouncing basketball rebounds higher than its initial drop height.
 - *Newton's Second Law / Trajectory Error:* The parabolic trajectory disappears (e.g., a thrown basketball or rock flies in a perfectly straight diagonal line without gravitational drop); a rock drifts down slowly like a feather, or a feather drops straight down heavily; an object naturally falling only under gravity falls in an S-shape trajectory; poured water flows in an S-shape mid-air; an object that should change its motion state under force remains completely static (e.g., a falling object suddenly hovers mid-air, or an object pushed off a table freezes in the air); an object is pushed or steered by an "invisible force" (e.g., a ball rolls on its own, liquid stirs itself, a door opens autonomously, a pen writes by itself, an object suddenly levitates); objects on a tilted plate cannot be poured out.
 - *Anti-Gravity / Anti-Entropy:* A shattered object spontaneously reassembles itself (reversed playback); spilled water automatically retracts into the cup; water flows uphill.
 - *Equilibrium Violation:* The heavier end of a seesaw remains suspended in the air; wooden blocks or Jenga towers do not collapse when their supporting structures are removed.

(6) Constraint Violation

- **Definition:** The magnitude or nature of the interaction consequence mismatches the cause, or environmental/rigid-body constraints are breached.
- **Examples:**
 - *Thermodynamic / Environmental Interaction:* A candle burns steadily in a strong gale; ice or butter remains solid over an open flame; combustion occurs in an oxygen-free environment; a strong storm occurs (background trees bending violently), but a flag or a model's hair remains perfectly static like a statue; a flag remains motionless in the wind.
 - *Causal Imbalance / Magnitude Mismatch:* A falling feather triggers a massive water splash; a small rock thrown into water creates absolutely no ripples, or creates an impossibly huge splash; drinking from a cup does not decrease the water level; a kettle pours no water, yet the cup's water level rises; the sand level in the top half of an hourglass does not decrease; stirring ingredients fails to mix them, or the resulting mixture's property/color/state physically mismatches the inputs.
 - *Property Mismatch:* A hammer made of crumpled paper easily shatters a solid glass window; stirring videos exhibit incorrect material properties.
 - *Rigid-Body Failure:* A robotic arm phases through a solid wall; objects intersect or tools fail unphysically (e.g., colliding spheres pass directly through each other without rebounding; a tool like a spoon, knife, or hand penetrates a solid or liquid, but the target exhibits zero displacement or deformation).

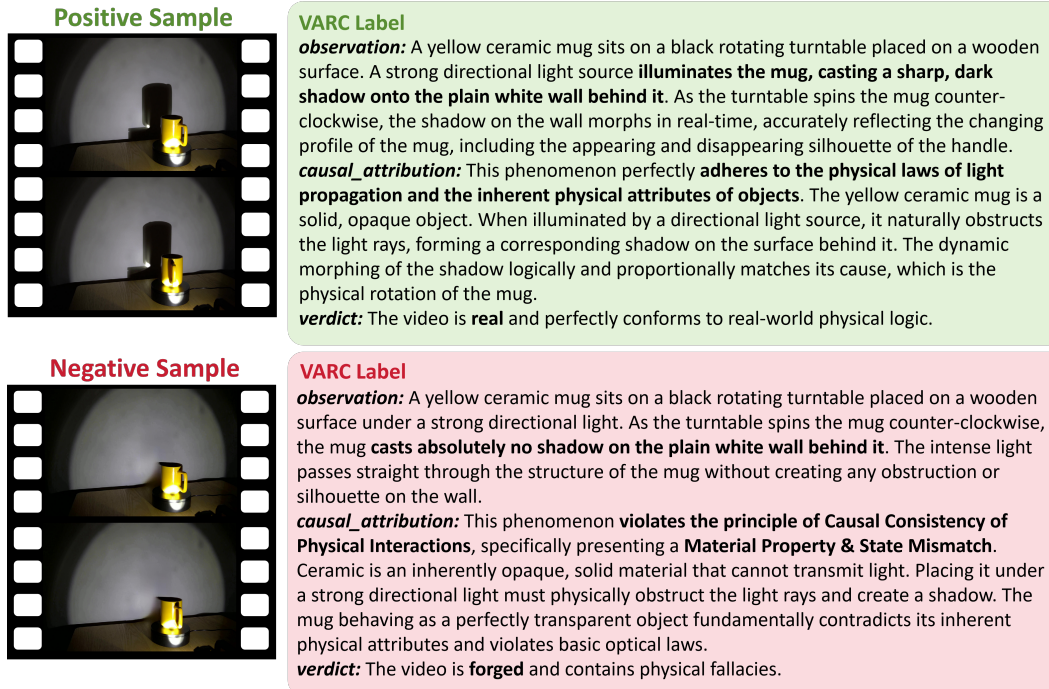


Figure 5: A real qualitative example from the PACC dataset illustrating the Constraint Violation sub-category. The figure displays a paired positive and negative video sample alongside their corresponding VARC labels. In the negative sample, the absence of a shadow despite a strong directional light violates fundamental optical laws and material properties (Property Mismatch). This structured format forces models to ground their physical attribution strictly in explicit visual observations.

A.2 Stream 2: Counter-Intuitive

This stream targets stereotypical fallacies. These samples are physically plausible but act as adversarial traps where expected events fail to occur, penalizing models for ignoring visual gaps and relying on semantic scripts.

(7) Near-Miss

- **Definition:** An object’s trajectory enters an interaction zone, but a clear spatial gap prevents physical contact, avoiding the expected chain reaction.
- **Examples:** A ball rolls at high speed toward dominoes but brushes past them by a millimeter without touching, leaving the dominoes static; a foot aggressively swings at a football but misses entirely, leaving the ball unmoved; a hammer swings toward glass but stops just before impact.

(8) Consequence Arrest

- **Definition:** The initiating action occurs (e.g., raising a hammer), but the process is unexpectedly interrupted or lacks sufficient intensity, blocking the semantically expected physical consequence (e.g., breaking, spilling).
- **Examples:** A hammer forcefully strikes a glass pane, but due to insufficient force, the glass remains perfectly intact; a hand tilts a water cup, but due to an insufficient tilt angle or surface tension, the water does not spill.

To concretely illustrate the rigorous annotation structure of PACC, Figure 5 presents a complete qualitative example from the *Constraint Violation* sub-category. As demonstrated, each adversarial pair is accompanied by a meticulously crafted VARC label. By enforcing a strict sequence of forced

observation, causal attribution, and final verdict, this format prevents the model from relying on semantic shortcuts. In this specific negative sample, the model is penalized if it ignores the explicit visual fact (the absence of a shadow) and instead hallucinates an outcome based on the statistical prior of a mug under a spotlight.

B Experimental and Training Details

This section provides comprehensive details regarding our computational setup, hyperparameters, and evaluation protocols to ensure full reproducibility of our results.

B.1 Hardware and Compute Resources

All experiments, including dataset synthesis, model fine-tuning, and evaluation, were conducted on a single compute node equipped with $8 \times$ NVIDIA RTX A6000 GPUs. The entire Supervised Fine-Tuning (SFT) process of our Physics-Anchored Reasoner (PhyAR) on the PACC dataset for 3 epochs required approximately 4 hours of total compute time. This lightweight computational footprint highlights the efficiency of our Visual-Anchored Reasoning Chain (VARC) coupled with the paired optimization strategy.

B.2 Training Hyperparameters

We build PhyAR upon the VideoLLaMA3-7B base model. To optimize memory usage while preserving representation quality, the LLM backbone is loaded using 4-bit NormalFloat (NF4) quantization with double quantization enabled, while all forward computations are performed in `bf16` precision. We also employ FlashAttention-2 to accelerate training dynamics.

During fine-tuning, the vision encoder is strictly frozen. We apply Low-Rank Adaptation (LoRA) to all linear layers (Q, K, V, O, and MLP projections) of the LLM backbone, as well as to the multimodal projection layer. We utilize the 8-bit AdamW optimizer to further minimize optimizer state memory. The paired data optimization is implemented using a gradient accumulation step of 4, effectively ensuring that each backpropagation update firmly grounds the contrastive gradients between positive and negative pairs. Detailed hyperparameters are summarized in Table 5.

Table 5: **Hyperparameters for PhyAR Supervised Fine-Tuning.**

Hyperparameter	Value
Base Model	VideoLLaMA3-7B
Hardware	$8 \times$ NVIDIA RTX A6000
Training Epochs	3
Learning Rate	$5e-5$
LR Scheduler	Cosine Annealing
Optimizer	8-bit AdamW
LLM Fine-tuning	LoRA ($r = 16, \alpha = 32, \text{dropout}=0.1$)
Projector Fine-tuning	LoRA ($r = 16, \alpha = 32, \text{dropout}=0.1$)
Precision	4-bit NF4 (Backbone) / <code>bf16</code>
Gradient Accumulation Steps	4

B.3 Baseline Evaluation Setup

To ensure strict reproducibility and entirely eliminate variance caused by generation stochasticity, all models (including PhyAR and all baselines) are evaluated under a strictly deterministic setting. Specifically, we enforce greedy decoding by setting `do_sample=False` and `temperature=0.0`. The `max_new_tokens` limit is set to 2048 to safely accommodate the detailed Chain-of-Thought (CoT) reasoning outputs mandated by the VARC prompt. For visual inputs, all models uniformly sample 16 frames per video. For text generation evaluation, we adopt the LLM-as-a-judge paradigm. The complete judge prompt and detailed 1-5 scoring rubric are provided in Appendix D.

C Broader Impacts

Positive Impacts. The introduction of the Programmatic Adversarial Curriculum (PACC) and the Visual-Anchored Reasoning Chain (VARC) protocol aims to significantly advance the development of physically grounded AI systems. By systematically exposing the rationalization fallacies and physical hallucinations in current Video Large Language Models (Video-LLMs), our work provides a critical stepping stone toward robust World Models. This is particularly vital for safety-critical domains such as Embodied AI, autonomous driving, and robotics, where relying on models with flawed physical intuitions could lead to catastrophic real-world failures. Furthermore, the VARC protocol enhances model interpretability by forcing AI systems to explicitly verbalize their visual evidence before drawing causal conclusions, fostering greater transparency and trust in AI-assisted decision-making.

Potential Risks and Mitigations. Despite its intended diagnostic purposes, the methodology behind constructing PACC involves the synthesis of high-fidelity videos depicting specific physical events and anomalies. There is an inherent dual-use risk: the advanced video generation pipelines utilized to create these adversarial samples could be co-opted by malicious actors to produce convincing deepfakes or visually plausible misinformation. To mitigate these risks, we strongly advocate for the mandatory integration of robust watermarking mechanisms in all generative models to ensure digital provenance. Moreover, datasets like PACC can inversely serve as valuable training grounds for developing sophisticated deepfake detection algorithms—systems capable of identifying forged media based on fundamental physical inconsistencies rather than merely relying on pixel-level artifacts.

D Complete Prompt Templates

This section provides the exact text prompts used across our data generation pipeline and evaluation framework. To ensure optimal model prediction stability and avoid interference from formatting artifacts, the prompts are fed into the models as pure text, stripped of markdown symbols.

D.1 Pipeline Stage 1: Visual Fact Anchoring & Target Fallacy Generation

This prompt is utilized to extract objective visual facts from the source video and determine the most appropriate physical fallacy scenario based on the provided taxonomy.

Role & Core Function

You are an expert in Computer Vision (CV) and Generative AI, specializing in video semantic understanding and synthetic data creation.

Core Guidelines:

Strict Adherence: You must carefully read and strictly execute the Category Definition and Reasoning Pipeline provided by the user.

Visual Evidence Only: All analysis must be strictly based on the visible pixel content of the video. Do NOT hallucinate objects or actions not present.

No Subjectivity: In the captioning phase, strictly describe what is happening. Do NOT infer why (physics laws), intent, or emotions.

Contextual Adaptation: The examples in "Typical Scenarios" are illustrative references. You must strictly select one scenario and apply its physical violation logic to the actual subjects and actions in the Input Video.

Input Context

Context 1: Category Definition: The provided examples for each sub-category are illustrative, not exhaustive. You must deeply understand the Core Criterion.

Context 2: Input Video: The video file to be analyzed.

Reasoning Pipeline (Chain-of-Thought)

Perform the following 3 steps in a single logical flow:

Step 1: Visual Fact Anchoring

Basis: The Input Video.

Task A (Caption): Generate a strictly objective visual description. Focus ONLY on Subjects, Actions, and Environment. Constraint: Prohibition on explaining "why".

Task B (Style & Camera): Extract visual style and camera movement information.

Step 2: Fallacy Scenario Construction

Basis: Input Video + Step 1 Caption + Category Definition.

Polarity Check: Determine if the input is [Real] or [Fake]. Default is Real.

Task: Analyze the video content to determine the most suitable physics fallacy implementation.

1. Select the most appropriate Typical Scenario.

2. Output a Target Fallacy Scenario that clearly describes how the fallacy manifests.

Step 3: Generation Method Decision

Basis: Input Video + Step 2 Target Scenario + Modification Principles.

Principle for [Manual_CV_Edit]: Select this if the Target Fallacy Scenario can be achieved by rearranging existing pixels, removing objects, or layering.

Principle for [AI_Generation]: Select this if the Target Fallacy Scenario requires synthesizing new pixels or altering internal object properties.

Task: Analyze the technical requirements and select the Generation Method.

Output Format

Return a single valid JSON object.

```
{
  "visual_fact_caption": "String.",
  "visual_style_and_camera": "String.",
  "input_polarity": "Real OR Fake",
  "selected_typical_scenario": "String.",
  "target_fallacy_scenario": "String.",
  "reasoning_for_method": "String.",
  "generation_method": "Manual_CV_Edit OR AI_Generation"
}
```

D.2 Pipeline Stage 2: Video Generation Prompt Construction

Based on the outputs of Stage 1, this prompt constructs highly constrained instructions for the video generation model to synthesize the adversarial negative sample.

Dynamic Inputs

Visual Frames: [Input: 16 extracted frames from the original video]

Camera & Style: [Input: Extracted visual style and camera movement]

Original Caption: [Input: Strict objective description of the original action]

Target Fallacy Scenario: [Input: Detailed description of the target physics violation]

Core Task & Directives

Based on the inputs, write a highly precise English prompt for a video generation model to generate the Target Fallacy Scenario.

Establish Baseline & Execute Replacement: The prompt must use the Original Caption as the realistic baseline, but completely replace the logical outcome with the absurd events described in the Target Fallacy Scenario.

Absolute Forcing Principle: Force the video model to prioritize the Target Fallacy Scenario. You are strictly prohibited from attempting to "correct" these phenomena.

Core Prompting Rules

Structural Front-loading: Place the camera movement or visual style at the beginning.

Strong Explicit Negation & Contrast: Use strong negative words (e.g., NOT, completely misses) to definitively break semantic priors.

Temporal Slicing Expression: For sudden state changes, use clear temporal anchors

(e.g., Trigger:, Phase 2...).

Summary Qualitative Label: Conclude with a brief declarative sentence labeling the anomaly (e.g., A clean miss.).

Output Constraint

Return a single valid JSON object.

```
{
  "generated_video_prompt": "String. The final constructed English prompt."
}
```

D.3 Pipeline Stage 3: VARC SFT Data Synthesis

This prompt acts as the final aggregator, compiling the factual and counterfactual elements into the structured Visual-Anchored Reasoning Chain (VARC) format used for fine-tuning. For different adversarial categories, the respective physics definitions from Appendix A are dynamically injected into the PACC Category Dictionary variable.

Input Information

Visual Fact Caption: {Insert visual_fact_caption here}

Target Fallacy Scenario: {Insert target_fallacy_scenario here}

Fallacy Category: {Insert selected_typical_scenario here}

Task Objective and Rules

You are an expert data annotator. Construct a pair of structured Three-Step CoT (Physically Plausible vs. Physically Implausible) for training Video-LLMs.

1. Observation

Rule: Generate a strictly objective visual description. Focus ONLY on Subjects, Actions, and Environment. No causal speculations.

Positive Sample Observation: Base this entirely on the Visual Fact Caption.

Negative Sample Observation: Integrate the abnormal actions from the Target Fallacy Scenario into the Visual Fact Caption.

2. Attribution

Rule: Use the PACC Category Dictionary below to explain physical adherence.

Positive Sample Attribution: Explain which fundamental laws the video adheres to.

Negative Sample Attribution: Point out which physical law the Target Fallacy Scenario violates.

3. Verdict

Positive Sample Verdict: Summarize that the video is real and conforms to logic.

Negative Sample Verdict: Summarize that the video is forged and contains fallacies.

PACC Category Dictionary

{Dynamically injected definitions based on the selected fallacy category}

Output Requirements

Strictly return the output in JSON format.

```
{
  "positive_sample": {
    "observation": "...",
    "causal_attribution": "...",
    "verdict": "...",
    "sft_response": "Observation:... \n Attribution:... \n Verdict:..."
  },
  "negative_sample": {
    "observation": "...",
    "causal_attribution": "...",
    "verdict": "...",
  }
}
```

```

    "sft_response": "Observation:... \n Attribution:... \n Verdict:..."
  }
}

```

D.4 Evaluation: LLM-as-a-Judge Rubric

This prompt details the rigorous grading criteria used to evaluate model outputs during testing, ensuring a strict decoupling between the final predictive verdict and the logical soundness of the physical reasoning.

Evaluation Criteria

Compare the Model Output with the Ground Truth. You must strictly decouple the evaluation of the final verdict (Real/Forged) from the evaluation of the reasoning process. Output a strict JSON object.

CRITICAL RULE: The score MUST strictly align with the accuracy:

If accuracy = 0, the score MUST be 1 or 2.

If accuracy = 1, the score MUST be 3, 4, or 5.

1. "reasoning": (String) A step-by-step analysis comparing the entities, state transitions, and causal logic.
2. "accuracy": (Integer) 0 or 1. STRICTLY evaluate ONLY the final binary verdict. (1 if matches, 0 if contradicts). DO NOT let flawed reasoning lower the accuracy to 0. If the model guessed the right verdict for the wrong reasons, the accuracy MUST be 1.
3. "score": (Integer) 1 to 5. The reasoning quality score:
 - 1: (Requires accuracy=0) Wrong verdict, and severe hallucinations.
 - 2: (Requires accuracy=0) Wrong verdict, but correctly observed some entities.
 - 3: (Requires accuracy=1) Correct verdict, BUT reasoning is hallucinated (Right for the wrong reasons).
 - 4: (Requires accuracy=1) Correct verdict, reasoning basically matches Ground Truth with minor flaws.
 - 5: (Requires accuracy=1) Correct verdict, perfect alignment in causal reasoning.

Output Requirements

Output ONLY a valid JSON object.

```

{
  "reasoning": "...",
  "accuracy": 1,
  "score": 3
}

```